Human Molecular Genetics, 2017, Vol. 0, No. 0 1–14

doi: 10.1093/hmg/ddx016
Advance Access Publication Date: 13 January 2017
Original Article

ORIGINAL ARTICLE

Metformin restores the mitochondrial network and reverses mitochondrial dysfunction in Down syndrome cells

Antonella Izzo[1,†], Maria Nitti[1,2,†], Nunzia Mollo[1,†], Simona Paladino[1], Claudio Procaccini[3], Deriggio Faicchia[4], Gaetano Calì[3], Rita Genesio[1], Ferdinando Bonfiglio[5], Rita Cicatiello[1], Elena Polishchuk[6], Roman Polishchuk[6], Paolo Pinton[2], Giuseppe Matarese[1], Anna Conti[1,*] and Lucio Nitsch[1]

[1]Department of Molecular Medicine and Medical Biotechnology, University of Naples Federico II, 80131 Naples, Italy, [2]Department of Morphology, Surgery and Experimental Medicine, University of Ferrara, 44100 Ferrara, Italy, [3]Institute of Experimental Endocrinology and Oncology, National Research Council, 80131 Naples, Italy, [4]Department of Translational Medical Sciences, University of Naples Federico II, 80131 Naples, Italy, [5]Department of Biosciences and Nutrition, Karolinska Institutet, 17177 Stockholm, Sweden and [6]Telethon Institute of Genetics and Medicine (TIGEM), 80078 Pozzuoli, Italy

*To whom correspondence should be addressed at: Department of Molecular Medicine and Medical Biotechnology, University of Naples Federico II, Via Pansini 5, Naples 80131, Italy. Tel: +39 0817463621; Fax: +39 0817463656; E-mail: anconti@unina.it
†The authors wish it to be known that, in their opinion, the first three authors should be regarded as joint First Authors

Abstract

Alterations in mitochondrial activity and morphology have been demonstrated in human cells and tissues from individuals with Down syndrome (DS), as well as in DS mouse models. An impaired activity of the transcriptional coactivator *PGC-1α/PPARGC1A* due to the overexpression of chromosome 21 genes, such as *NRIP1/RIP140*, has emerged as an underlying cause of mitochondrial dysfunction in DS. We tested the hypothesis that the activation of the *PGC-1α* pathway might indeed reverse this mitochondrial dysfunction. To this end, we investigated the effects of metformin, a *PGC-1α*-activating drug, on mitochondrial morphology and function in DS foetal fibroblasts. Metformin induced both the expression of *PGC-1α* and an augmentation of its activity, as demonstrated by the increased expression of target genes, strongly promoting mitochondrial biogenesis. Furthermore, metformin enhanced oxygen consumption, ATP production, and overall mitochondrial activity. Most interestingly, this treatment reversed the fragmentation of mitochondria observed in DS and induced the formation of a mitochondrial network with a branched and elongated tubular morphology. Concomitantly, cristae remodelling occurred and the alterations observed by electron microscopy were significantly reduced. We finally demonstrated that the expression of genes of the fission/fusion machinery, namely *OPA1* and *MFN2*, was reduced in trisomic cells and increased by metformin treatment. These results indicate that metformin promotes the formation of a mitochondrial network and corrects the mitochondrial dysfunction in DS cells. We speculate that alterations in the mitochondrial dynamics can be relevant in the

Received: November 8, 2016. **Revised:** December 16, 2016. **Accepted:** December 21, 2016

pathogenesis of DS and that metformin can efficiently counteract these alterations, thus exerting protective effects against DS-associated pathologies.

Introduction

Down syndrome (DS), due to either full or partial trisomy of chromosome 21 (Hsa21), is characterized by a highly complex and variable phenotype (1). The most important consequence of Hsa21 trisomy (TS21) is a neural developmental delay, associated with some impairment in cognition, language, learning and memory (2–4). Other DS common features include heart defects, hypotonia and metabolic and immune disorders. Several studies in different animal models (5), as well as in human subjects (6–8) have suggested that the mitochondrial abnormalities might be critically associated with the pathogenesis of DS features.

DS tissues and cells exhibit functional and structural mitochondrial abnormalities including reduced respiratory capacity, mitochondrial membrane potential, ATP production, decreased oxido-reductase activity and impaired mitochondrial dynamics. Interestingly, mitochondrial defects are present in all DS cells analysed in a culture so far, including neurons, astrocytes, pancreatic beta cells, smooth muscle cells and lymphocytes (9,10). Foetal and adult TS21 fibroblasts show a significant increase in ROS, in addition to a decreased catalytic efficiency of proteins involved in ATP production and a decreased oxygen consumption rate (OCR) (8,11–14). Furthermore, a substantial alteration in mitochondrial morphology was observed in primary cultures of TS21 astrocytes and neurons with increased fragmentation of the mitochondrial network (15). Electron microscopy of TS21 foetal fibroblasts also revealed that a significant number of mitochondria have irregular shape, evident breaks, mainly of inner membranes, and alterations in the pattern of cristae (8).

Thus, mitochondrial dysfunction may contribute to several common phenotypes present in DS subjects namely heart defects, hypotonia, immune system alterations, increased incidence of diabetes, obesity and Alzheimer's disease (AD). Expression profiling studies have revealed a substantial downregulation of nuclear-encoded mitochondrial genes (NEMGs) in TS21 foetal tissues (16,17). The Hsa21 gene *NRIP1/RIP140* (nuclear receptor interacting protein 1), which is overexpressed in DS tissues, has been demonstrated to be a repressor of nuclear-encoded mitochondrial genes as well as to play a key role in mitochondrial dysfunction and biogenesis in DS (18). Two other Hsa21 genes, namely *DYRK1A* and *DSCR1/RCAN1*, play important roles in the calcineurin/*NFAT* pathway, which affects mitochondrial activity and morphology (19). In addition, it was recently reported that the Hsa21 miR-155-5p affects mitochondrial biogenesis by targeting mitochondrial transcription factor A (20). Interestingly, the common denominator of all of these mechanisms is the transcriptional coactivator *PGC-1α/PPARGC1A* (peroxisome proliferator-activated receptor gamma coactivator 1 alpha), a master regulator of mitochondrial biogenesis. *PGC-1α* is dowregulated at both the mRNA and protein levels in TS21 human foetal fibroblasts (8), and its expression level is restored after attenuation by siRNA of the *NRIP1* mRNA levels (18).

PGC-1α binds to the transcription factors *ERRα, NRF-1* and *NRF-2* and increases their expression, creating positive feedback loops (21). *PGC-1α* activity may be modulated by post-translational events through changes in *SIRT1/AMPK/PKA* signalling (21). Direct phosphorylation of the PGC-1α protein by AMPK is required for PGC-1α-dependent induction of the *PGC-1α* promoter (21,22). AMPK also regulates SIRT1 activity (23), which in turn stimulates PGC-1α activity through its deacetylation (24).

Thus, the induction of *PGC-1α* might represent a potential therapeutic target for reversing mitochondrial abnormalities in DS. This approach is reinforced by our previous results demonstrating a direct correlation between *PGC-1α* expression and mitochondrial function in TS21 fibroblasts (8,18).

On the basis of these considerations, we are pursuing a strategy to correct mitochondrial alterations with the final aim of improving the DS phenotype. To this end, we used human trisomic foetal fibroblasts, in which we have thoroughly characterized the mitochondrial phenotype, to determine whether the administration of metformin, a PGC-1α activator, would counteract the impairment of mitochondrial activity. We decided to use metformin because this drug is known (i) to induce the *PGC-1α* expression and activation via *AMPK* and *SIRT1* (25); (ii) to promote neurogenesis and enhance spatial memory formation in the normal adult mouse (26); (iii) to cross both the blood-brain and placental barriers (27,28); and (iv) to be already in use but for different diseases.

In this study, we evaluated the effects of metformin treatment on mitochondrial metabolism as well as on the mitochondrial network and ultrastructure in the human cell model of DS in which we have fully characterized the mitochondrial phenotype (8,18). We determined for the first time that metformin restores mitochondrial morphology and counteracts the impairment of mitochondrial function.

Results

The *PGC-1α* signalling pathway is a target of the drug metformin

We previously reported that PGC-1α mRNA and protein levels are reduced by 40–50% in human fibroblasts from DS foeti (DS-HFFs) when compared with their non-trisomic counterparts (N-HFFs) (8). Because metformin treatment was demonstrated to induce *PGC-1α* expression as well as to activate the *PGC-1α* function in different biological contexts (25), we decided to assess whether *PGC-1α* is a target of metformin also in DS-HFFs. To this end, we analysed the mRNA and protein levels of PGC-1α in metformin-treated cells. Two drug concentrations were used, 0.05 and 0.5 mM, according to the literature (29) and results of preliminary experiments (Supplementary Material, Fig. S1). DS-HFFs treated for 72 h showed a significant increase in *PGC-1α* expression, at both the mRNA (Fig. 1A) and protein levels (Fig. 1B), when compared with untreated control cells.

To verify whether metformin treatment resulted in activation of the *PGC-1α* signalling pathway, we also measured the mRNA levels of two transcription factors known to be affected by *PGC-1α* activity: *NRF-1*, which is induced by *PGC-1α* in a dose-dependent manner (30), and the mitochondrial transcription factor A (*TFAM*) (20), a critical regulator of mitochondrial gene transcription and mtDNA replication, which is positively regulated by *NRF-1* expression (31). The mRNA levels of both *NRF-1* and *TFAM* are lower in DS-HFFs vs N-HFFs, as reported by Piccoli *et al.* (8). Metformin treatment for 72 h induced an

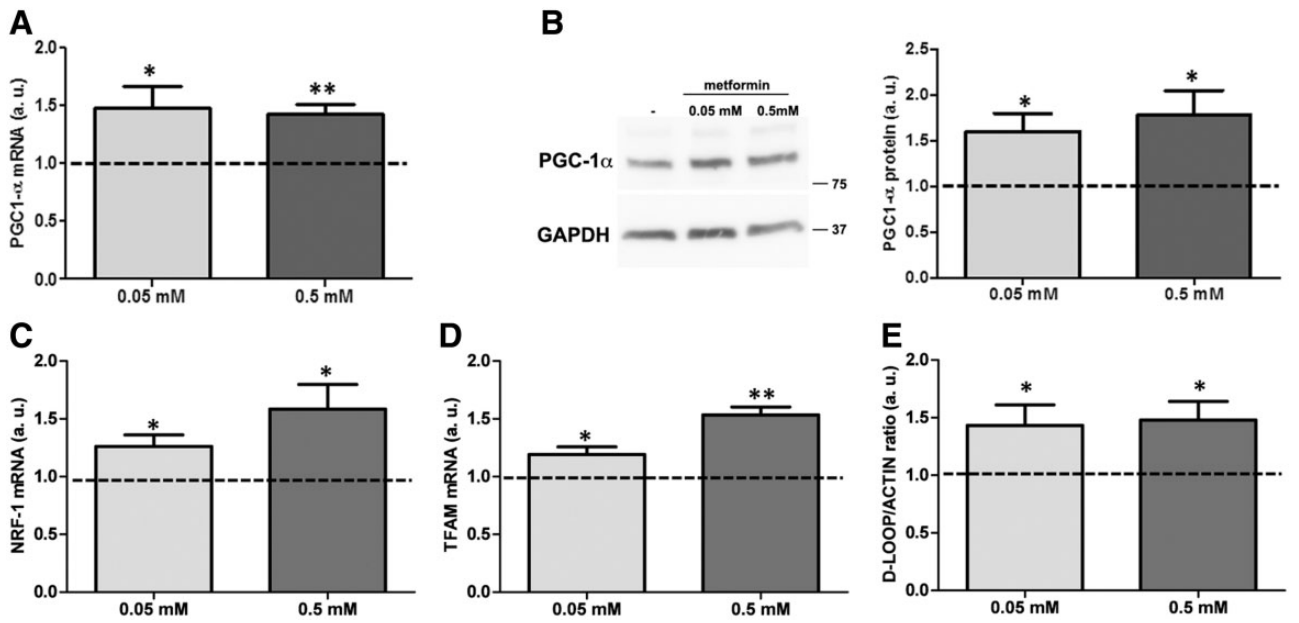

Figure 1. Metformin treatment increases *PGC-1α*, *NRF-1* and *TFAM* expression and mtDNA content in DS-HFFs. DS-HFFs were treated with 0.05 mM or 0.5 mM metformin for 72 h. (**A**) *PGC-1α* mRNA expression by qRT-PCR. (**B**) PGC-1α protein detected by immunoblotting in total protein fractions. Representative immunoblotting of PGC-1α and densitometric analysis of three different experiments is shown. GAPDH was used as a loading control. Metformin induces both *PGC-1α* mRNA and protein expression in DS-HFFs. (**C**) *NRF-1* and (**D**) *TFAM* mRNA expression. The expression of both genes is increased by drug treatment. (**E**) Ratio between the mtDNA marker *D-LOOP* and the nuclear DNA marker *ACTIN* indicates an increase of mtDNA after metformin treatment. Results are expressed as relative mean values ± SEM of three DS cell cultures treated with metformin, compared with untreated cells (set equal to 1). $^{*}P \leq 0.05$; $^{**}P \leq 0.01$; a.u. = arbitrary units.

increase in the mRNA levels of both *PGC-1α* target genes (Fig. 1C and D).

Because mtDNA replication is controlled by *PGC-1α* (21), we also analysed the correlation between *PGC-1α* expression/activity and the amount of mtDNA in metformin-treated cells. It has been previously demonstrated that the amount of mtDNA is lower in trisomic samples than in non-trisomic ones (8). A direct correlation between *PGC-1α* expression/activity and the amount of mtDNA was observed in metformin-treated DS cells, as demonstrated by the increase in the *D-LOOP/ACTIN* ratio in treated DS-HFFs vs untreated controls (Fig. 1E).

Metformin increases the respiratory activity of trisomic cells

To assess whether the induction of the *PGC-1α* signalling pathway is associated with the rescue of mitochondrial function, we measured the oxygen consumption rate (OCR) in metformin-treated DS-HFFs. We have previously demonstrated that DS-HFFs, together with the downregulation of NEMGs, manifest a reduced OCR (8).

In order to assess the OCR, we used the XF^{e}96 Extracellular Flux Analyzer (Seahorse Bioscience, Billerica, MA, USA). DS-HFFs were compared with N-HFFs with respect to three key parameters of mitochondrial function: basal OCR, ATP turnover and maximal respiration. Basal OCR was decreased in DS-HFFs (≈55% inhibition) when compared with N-HFFs (Fig. 2A, "Basal"). The OCR related to ATP production, calculated as the difference between basal and Oligomycin-induced OCR, was decreased in DS-HFFs (≈58% inhibition) (Fig. 2A, "ATP-linked"), as was the OCR in the presence of the carbonyl cyanide 4-phenylhydrazone (FCCP), a mitochondrial electron chain uncoupler. The maximal respiratory capacity, calculated as the difference between the FCCP-stimulated OCR and the OCR after inhibition with Antimycin-A and Rotenone (Fig 2A, "Maximal") was reduced in DS-HFFs (≈58% inhibition) when compared with N-HFFs. All of these data were in agreement with those previously reported, which had been obtained using different methodology (8).

To test whether metformin could affect cellular metabolism, we measured the bioenergetic profiles of DS-HFFs treated with metformin for 72 h. Interestingly, metformin treatment restored mitochondrial respiration in DS-HFFs, as indicated by the increase in basal OCR (Fig. 2B, "Basal"), OCR related to ATP production (Fig. 2B,"ATP-linked") and maximal respiratory capacity (Fig. 2B, "Maximal").

Cellular ATP concentration is increased by metformin treatment

As the XF^{e}96 Extracellular Flux Analyzer provides only an indirect measure of ATP production, we determined the basal cellular ATP concentration using a mitochondrially targeted luciferase protein in intact cells as previously described (18). We first compared DS-HFFs with N-HFFs, demonstrating a decrease in basal ATP content in trisomic cells (Fig. 3A). Because basal ATP content is highly dependent on the abundance of transfected luciferase, we determined, by immunoblot assay, the amount of the luciferase transduced under our experimental condition. We found that the levels of luciferase protein transduced in DS-HFFs were comparable to those detected in N-HFFs (Fig. 3B).

Intracellular ATP content was then investigated after metformin treatment in trisomic cells. Metformin induced a significant increase in ATP content in DS-HFFs (Fig. 3C), in agreement with the XF^{e}Analyzer results.

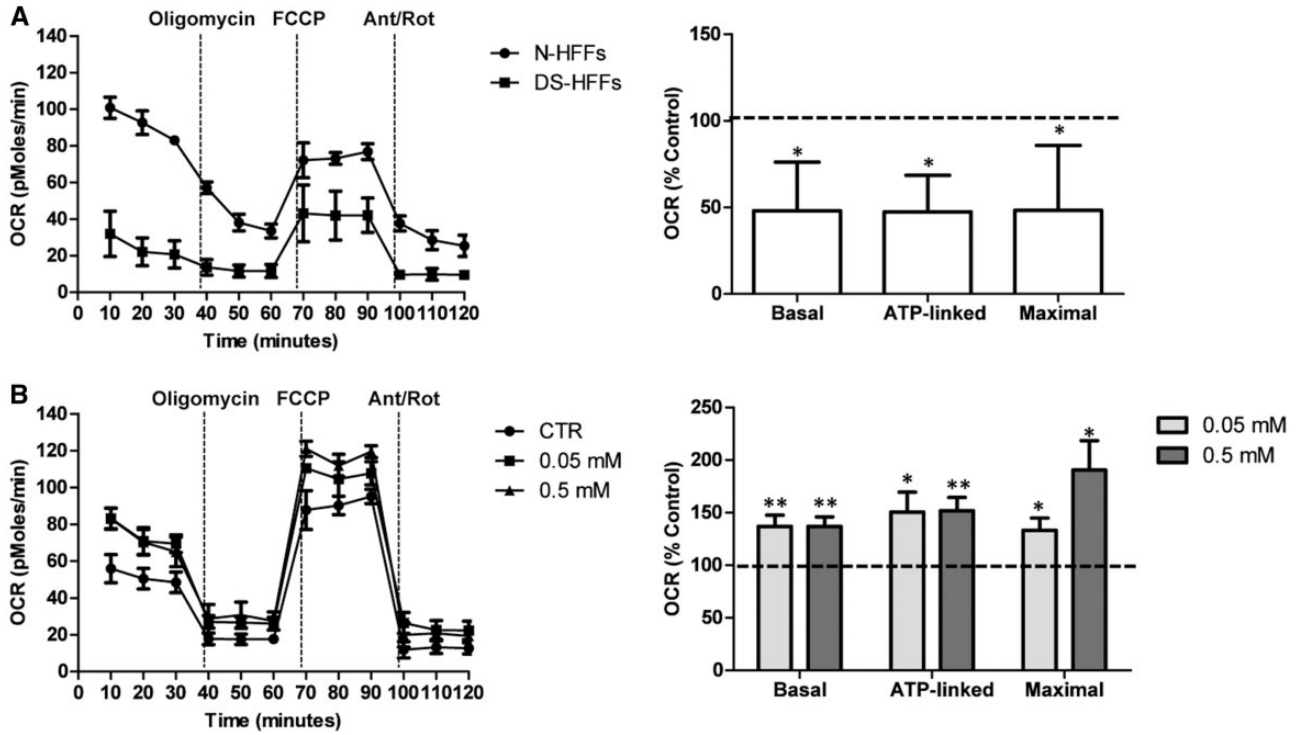

Figure 2. Metformin increases OCR in DS-HFFs. (**A**) OCR measurement in DS-HFFs vs N-HFFs. Representative curves of OCR in N-HFF and DS-HFF cells (single cell culture in triplicate) obtained in basal condition and after consecutive addition of Oligomycin 5 μM, FCCP 1.5 μM and Antimycin-A/Rotenon 1 μM (Ant/Rot) (left panel). The indices of mitochondrial respiratory functions (basal OCR, ATP-linked and Maximal OCR) are significantly decreased in DS-HFFs when compared with N-HFFs (right panel). The bars show the mean values ± SEM of four DS cell cultures compared with four N-HFFs (set equal to 100). (**B**) OCR measurement after 72 h of metformin treatment at 0.05 or 0.5 mM concentrations in DS-HFFs. Representative curves of OCR in treated DS-HFF cells (single cell culture in triplicate) (left panel). Basal, ATP-linked and Maximal OCR are significantly increased in DS-HFFs upon metformin treatment (right panel). Results are expressed as relative mean values ± SEM of four trisomic cell lines treated with metformin, compared with untreated cells (set equal to 100). *$P \leq 0.05$; **$P \leq 0.01$.

Metformin increases mitochondrial membrane potential (mΔΨ)

The mΔΨ was determined by confocal microscopy using the specific mitotropic probe tetramethylrhodamine methyl ester (TMRM), a red fluorescent dye sensitive to membrane potential changes. Fluorescence intensity was measured and normalized by basal fluorescence intensity levels obtained treating cells with FCCP, an uncoupler of oxidative phosphorylation (see also Methods).

Using this method, DS-HFFs showed a significant 50% decrease in TMRM fluorescence when compared with N-HFFs (Fig. 4A and B).

To evaluate the effects of metformin, we compared treated DS-HFFs with untreated controls (Fig. 4C). A significant difference in TMRM-related fluorescence was observed in metformin-treated cells at a concentration of 0.5 mM. The increase in fluorescence at the 0.05 mM concentration was not significant (Fig. 4D).

To obtain additional evidence that metformin improves mitochondrial activity, we incubated metformin-treated DS-HFFs with MitoTracker Red dye, a reagent that stains mitochondria in live cells according to their membrane potential. A significant difference was observed in MitoTrackerRed-related fluorescence in metformin-treated cells at a concentration of 0.5 mM (Fig. 5A and B).

Metformin promotes mitochondrial network formation

It is becoming increasingly clear that mitochondrial dynamics, as well as ultrastructure and volume, are mechanistically linked to mitochondrial function (32).

To determine if metformin affects mitochondrial morphology, we examined the overall organization of the mitochondrial network at the confocal microscope by looking at the distribution of a green fluorescent protein targeted to mitochondria (mtGFP).

N-HFFs and DS-HFFs were first compared. The N-HFF mitochondrial network exhibited a branched, tubular morphology, whereas that of DS-HFFs appeared fragmented with many small and short mitochondria (Fig. 6A). The mitochondrial number was higher in DS-HFFs (Fig. 6B), whereas their average volume was significantly decreased (Fig. 6D). Total mitochondrial volume was not significantly changed (Fig. 6C).

We then investigated whether metformin treatment affected the mitochondrial network in DS-HFFs. Confocal microscopy analysis revealed a full rescue of the tubular morphology of mitochondria in metformin-treated DS-HFFs that formed a network closely resembling that of non-trisomic cells (Fig. 6E). The mitochondrial number was decreased (Fig. 6F) and the total volume as well as the individual mitochondrial volume was increased (Fig. 6G and H).

Metformin reverses mitochondrial ultrastructure abnormalities

The ultrastructure of mitochondria varies considerably in relation to the cell's physiological and pathological state (32). Ultrastructural alterations are frequently associated with mitochondrial dysfunction as described for different human diseases (32).

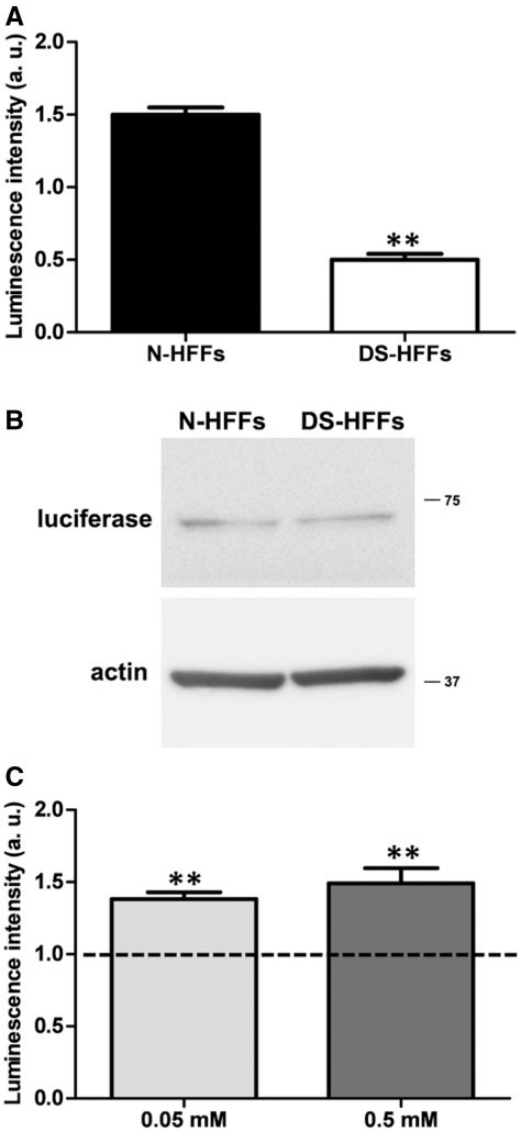

Figure 3. Metformin treatment of DS-HFFs increases ATP production. (**A**) Basal ATP in DS-HFFs versus N-HFFs, measured by a luciferase probe. The bars show the mean values ± SEM of a comparative analysis between three euploid and three trisomic cell lines. A significant ATP decrease is observed in DS-HFFs vs N-HFFs. (**B**) Representative immunoblot of luciferase protein in N-HFFs and DS-HFFs transfected with a mitochondrially targeted luciferase probe and cultured in complete medium for 72 h. Actin was used as loading control. (**C**) ATP measurement after 72 h of metformin treatment in DS-HFFs. ATP content is significantly increased in DS-HFFs treated with metformin when compared with untreated control cells. The bars show relative mean values ± SEM for four DS cell cultures treated with metformin, compared with untreated cells (set equal to 1). $^{**}P \leq 0.01$; a.u.= arbitrary units.

In agreement with previous data (8), the mitochondria of DS-HFFs were significantly damaged in comparison with those of N-HFFs. Mostly, they exhibited reduced or damaged cristae, which were broken, shorter, concentric or highly swollen (Fig. 7A, arrowheads). In addition, giant mitochondria with intra-oedema were observed (Fig. 7A, arrows). The number of damaged mitochondria in DS-HFFs was 3.5 fold higher when compared with N-HFFs (≈90% in DS-HFFs vs ≈25% in N-HFFs) (Fig. 7B) and ≈40% of DS-HFFs mitochondria displayed intra-oedema in comparison with those of non-trisomic cells (≈6%) (Fig. 7C).

Furthermore, because the proper cristae structure correlates with the mitochondrial respiratory efficiency (32,33), we also evaluated the maximal width of cristae, as previously described (34). Whereas in N-HFFs the inner mitochondrial membranes are closely juxtaposed at the level of the cristae, they appeared more widely spaced in DS-HFFs, as evidenced by the white space between them (Fig. 7A). Trisomic cells presented mitochondria with significantly wider cristae (≈2-fold) compared with non-trisomic cells (Fig. 7D). In addition, whereas in N-HFFs only ≈15% of mitochondria displayed swollen cristae (mean maximal width >30 a.u.), in DS-HFFs approximately 60–90% of mitochondria presented this feature (Fig. 7E).

We then investigated whether metformin treatment could restore the mitochondrial morphological phenotype (Fig. 7F). Notably, with respect to untreated cells, DS-HFFs treated with 0.5 mM metformin for 72 h presented significantly fewer damaged mitochondria (≈40%) (Fig. 7G) as well as mitochondria with intra-oedema (≈5%) (Fig. 7H) and narrower cristae with width comparable to N-HFFs cells (Fig. 7I and J).

Metformin treatment affects the mitochondrial fission/fusion machinery

The core machinery that governs the dynamic functional mitochondrial network is regulated by, among others, genes that induce fusion, namely the inner mitochondrial membrane GTPase Optic Atrophy 1 *(OPA1)* and the outer mitochondrial membrane fusion GTPases Mitofusins 1 and 2 *(MFN1* and *MFN2)* (35–37). To investigate the molecular bases of the alteration of the mitochondrial network in trisomic cells and of its rescue by metformin treatment, we analysed the mRNA and protein expression of *OPA1*, *MFN1* and *MFN2* in trisomic and non-trisomic cells.

We found that *OPA1* and *MFN2*, but not *MFN1*, mRNA and protein expression was significantly downregulated in DS-HFFs vs N-HFFs (Fig. 8A and B). This correlates with the extensive fragmentation of mitochondria observed in trisomic cells (Fig. 6). No variation in the mRNA as well in the protein level of the mitochondrial fission protein DRP1 was observed between DS and euploid cells (Supplementary Material, Fig. S2). Following exposure to metformin, the levels of *OPA1* mRNA and overall protein rose strongly (Fig. 8C and D). We did not detect any difference at the MFN1 protein level, while a slight increase in its mRNA was observed (Fig. 8C and D). Unlike *MFN1*, both mRNA and protein expression of *MFN2* was increased upon metformin treatment (Fig. 8C and D). These results agree with the reduced fragmentation of the mitochondrial network observed in metformin-treated trisomic cells. They also indicate that the restoration of proper levels of *OPA1* and *MFN2* is sufficient to rescue the correct mitochondrial phenotype. Moreover, the increase in *OPA1* expression is consistent with the restoration of the proper structure of cristae as *OPA1*, in addition to its role in mitochondrial fusion, is involved in the maintenance and remodelling of cristae morphology (38,39).

Discussion

Increasing evidence suggests that mitochondrial dysfunction, consistently observed in DS cells, tissues and animal models, contributes to the generation of the DS phenotype, including intellectual disability (40) and other possible post-natal complications (41). Impaired mitochondrial function has been demonstrated to be the consequence of a decrease in *PGC-1α*

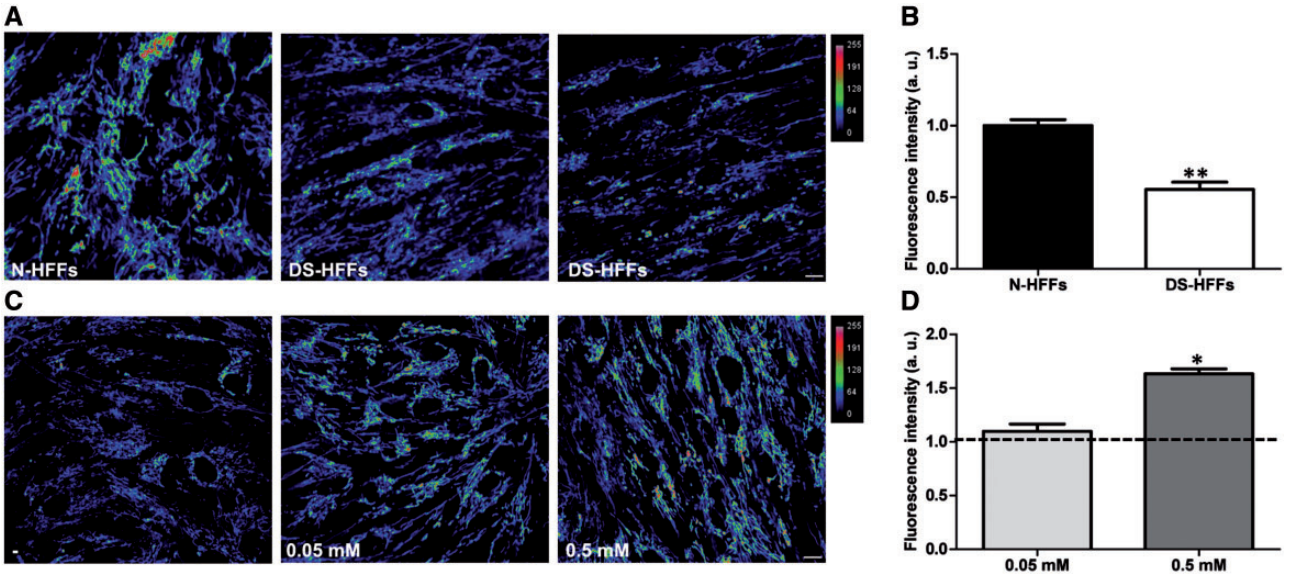

Figure 4. Membrane potential increases in metformin-treated DS-HFFs. (**A**) Representative confocal microscopy live cell imaging of TMRM fluorescence before FCCP in N-HFFs and DS-HFFs. (**B**) The bars show relative mean values ± SEM of fluorescence intensity per cell in four trisomic cell lines compared with four non-trisomic ones (set equal to 1). A significant decrease in fluorescence intensity is observed in DS-HFFs when compared with N-HFFs. (**C**) Representative confocal microscopy live cell imaging of TMRM fluorescence in untreated (-) DS-HFFs and those treated with metformin (0.05 and 0.5 mM). (**D**) The bars show relative mean values ± SEM of fluorescence intensity per cell in four trisomic cell cultures treated with metformin relative to untreated cells (set equal to 1). DS-HFFs show a significant increase in TMRM fluorescence upon 0.5 mM metformin treatment in comparison with untreated control cells. Fifty randomly selected cells for each sample/experimental condition were analysed. *$P \leq 0.05$; **$P \leq 0.01$; a.u. = arbitrary units.

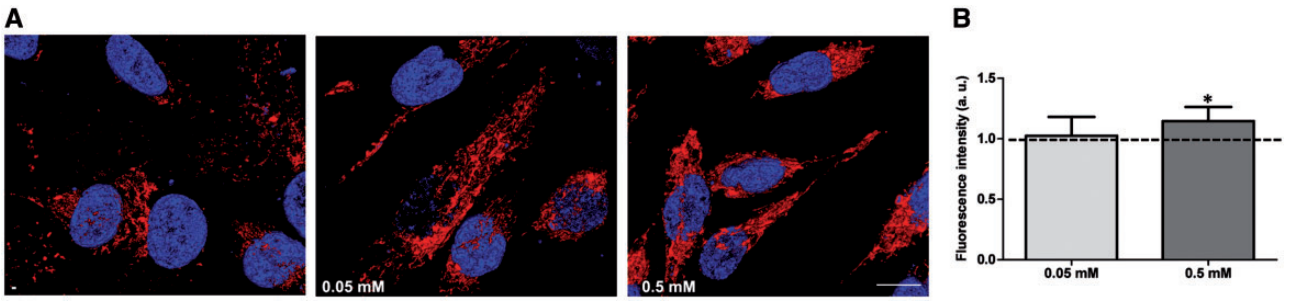

Figure 5. Mitochondrial function is rescued in metformin-treated DS-HFFs. (**A**) Confocal microscopy of the MitoTracker Red-related fluorescence in untreated DS-HFFs (-) and those treated with metformin (0.05 and 0.5 mM). Images correspond to the 3D reconstruction of Z-planes acquired from the top to the bottom of the cell. Scale bar 10 μm. (**B**) The bars show relative mean values ± SEM of fluorescence intensity per cell in four trisomic cell cultures treated with metformin, relative to untreated cells (set equal to 1). A significant increase in MitoTracker Red-related fluorescence is observed in metformin-treated DS-HFFs at a concentration of 0.5 mM. Fifty randomly selected cells for each sample/experimental condition were analysed. *$P \leq 0.05$; a.u. = arbitrary units.

expression (18). On these bases the activation of the *PGC-1α* pathway should therefore restore mitochondrial function and possibly improve the DS phenotype. We determined whether metformin, a drug that is known to induce *PGC-1α* activation (25), efficiently counteracts the mitochondrial dysfunction in DS.

Metformin induces the expression/activity of *PGC-1α*

To assess whether metformin enhances *PGC-1α* expression in trisomic cells, we analysed its mRNA transcript and protein levels in treated vs untreated cells.

We found that in trisomic cells both were significantly increased in a dose-dependent manner after metformin treatment. Crosstalk between nuclear and mitochondrial genomes is required to coordinate mitochondrial biogenesis (42,43). *NRF-1* and *TFAM*, two downstream targets of *PGC-1α*, are essential in this regard, as the former regulates the expression of multiple mitochondrial proteins encoded by nuclear genes, while the latter governs mitochondrial transcription. mRNA transcript levels of both *NFR-1* and *TFAM*, which are decreased in trisomic cells (8), were significantly increased after metformin treatment. The significant increase of mtDNA in treated trisomic cells was likely elicited by the induction of these genes. We conclude that metformin efficiently induces *PGC-1α* expression/activity, thus affecting its downstream pathway.

Metformin improves the whole energy status of trisomic cells

The bioenergetic deficit of trisomic cells involves both respiration and ATP synthesis due to a defect in the respiratory

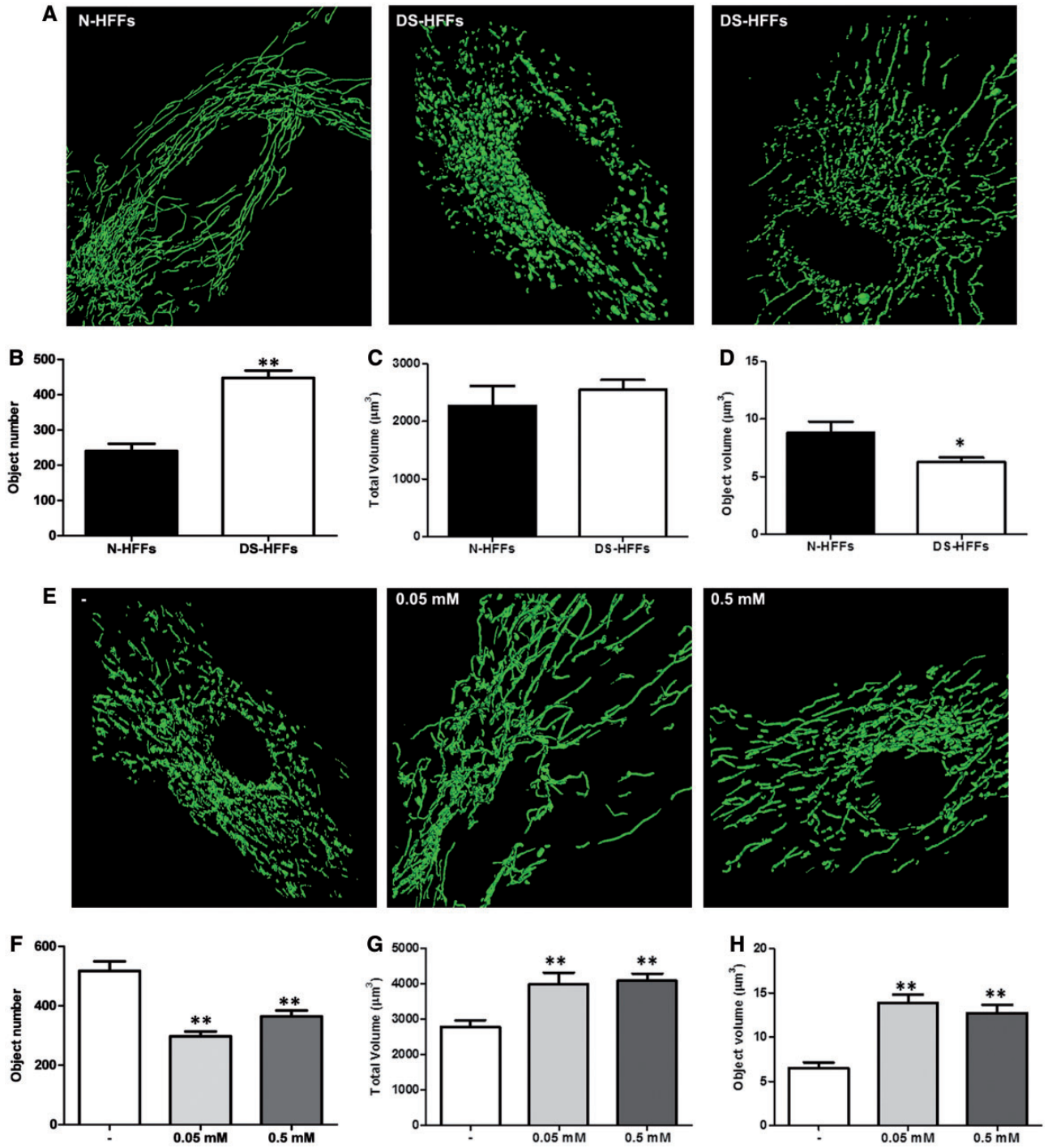

Figure 6. Metformin counteracts mitochondrial network fragmentation in treated DS-HFFs. (A) Representative images showing that the mitochondrial network is less fragmented in N-HFFs than in DS-HFFs. (B) The number of mitochondria is significantly higher in trisomic cells compared with non-trisomic cells. (C) The total volume is not significantly different. (D) The mitochondrial volume is significantly lower in DS cells compared with non-trisomic cells. The bars show mean values ± SEM of two non-trisomic and five trisomic cell cultures. (E) Representative images of the mitochondrial network in untreated DS-HFFs (-) and those treated with metformin. Fragmentation is decreased in DS-HFFs treated with metformin (0.05 or 0.5 mM) for 72 h. Metformin-treated DS cells show on average (F) a lower number of mitochondria, (G) an increase of total volume and (H) a higher individual mitochondrial volume compared with untreated cells. The bars show mean values ± SEM of five trisomic cell cultures (untreated or treated). Fifty randomly selected cells for each sample/experimental condition were analysed. *$P \leq 0.05$; **$P \leq 0.01$.

complex activity (8,13,14,44). We show here that basal OCR, OCR related to ATP production and maximal respiratory capacity measured in live intact cells are decreased in trisomic cells when compared with non-trisomic ones. An almost complete recovery of mitochondrial respiration is achieved in TS21 cells after metformin stimulation of the *PGC-1α* pathway: a significant increase in OXPHOS parameters is observed, including an increase in both OCR and ATP production.

PGC-1α also regulates genes encoding *ANT* (adenine nucleotide translocator) isoforms through different transcription

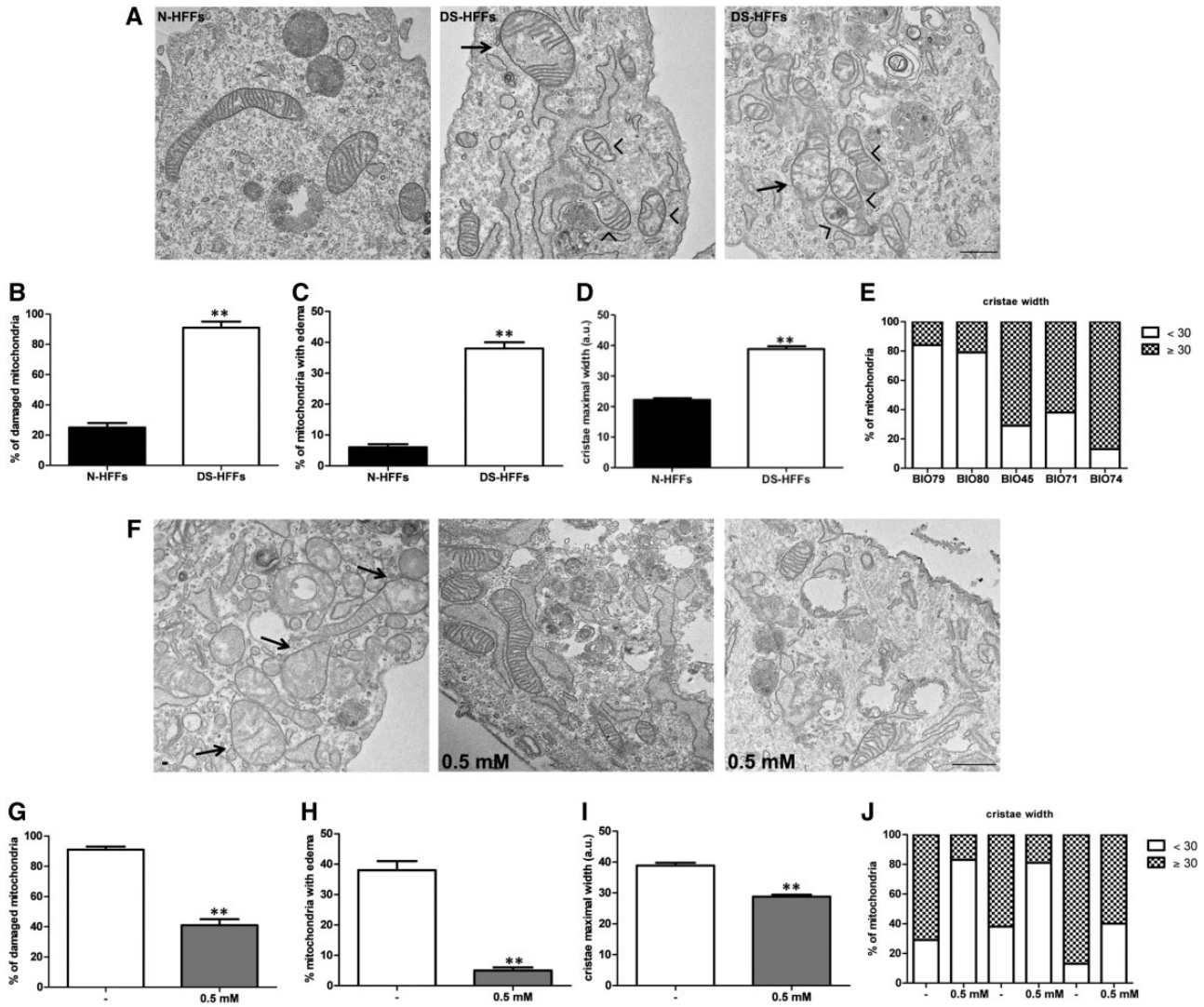

Figure 7. Mitochondrial ultrastructure is altered in DS-HFFs and is reversed upon metformin treatment. (**A**) Representative ultrastructural images of N-HFFs showing mitochondria with an intact morphology, without any particular changes in the structure, and of DS-HFFs showing damaged mitochondria characterized by a range of mitochondrial alternations (arrowheads). Giant mitochondria with intra-oedema are also observed (arrows). (**B**) The percentage of damaged mitochondria is significantly higher in trisomic cells compared with non-trisomic cells, as well as (**C**) the percentage of mitochondria with intra-edema. The bars show mean values ± SEM of two non-trisomic cells and three trisomic lines; $n > 80$ per cell line. (**D**) Mean cristae maximal width in N-HFFs versus DS-HFFs (see Material and Methods). DS-HFFs present mitochondria with significantly wider cristae (mean width: 38 a.u.) compared with N-HFFs (mean width: 22 a.u.). (**E**) The percentage of mitochondria with enlarged cristae (>30 a.u.) is higher in DH-FFs in comparison with NH-FFs. In D and E the bars show mean values ± SEM of two non-trisomic and three trisomic ones; $n > 20$ per sample. (**F**) Representative images of untreated and treated trisomic cells and quantitative analysis as above (**G–J**) are shown. Mitochondrial morphological abnormalities are restored in DS-HFFs treated with metformin (0.5 mM) for 72 h in comparison with untreated cells (-).The percentage of damaged mitochondria (G), of mitochondria with intra-edema (H) and of mitochondria with enlarged cristae (>30 a.u.) (J) is strongly reduced in treated vs untreated DS-HFFs. The mean cristae width is also reduced (mean width: 28 a.u.) (I). The bars show mean values ± SEM of three trisomic cell cultures (untreated or treated); $n > 60$ (G, H) or > 20 (I, J) per each cell line. Scale bar 1 μm. $^{**}P \leq 0.01$; a.u. = arbitrary units.

factors, depending on cell type (45). *ANT* isoforms were found to be downregulated in trisomic cells (17) and their expression was induced after *NRIP1* silencing and the consequent increase in *PGC-1α* expression (18). *ANT* genes are embedded in the inner mitochondrial membrane and facilitate the transport of ADP and ATP. They play a central role in OXPHOS as solute carriers and exchangers of matrix ATP for cytosolic ADP, thus providing mitochondrial energy to the cytosol (46). On these premises, *PGC-1α* induction could be the basis for both increased production and cytoplasmic transfer of ATP. As a possible consequence of the improvement in energy status, mΔΨ, which was decreased in DS foetal fibroblasts, showed a dose-dependent increase after metformin treatment. All of these effects are likely to be mediated by the induction of PGC-1α synthesis/activity, and of its downstream effectors, as also highlighted by Valenti *et al.* (47).

Metformin promotes mitochondrial network organization and restores mitochondrial morphology

There is a close relationship between the mitochondrial functional state and its dynamic network. Specifically, a proper dynamic balance between mitochondrial fusion and fission is fundamental to the function of this organelle (37). Cells with defective mitochondrial fusion machinery show dramatically

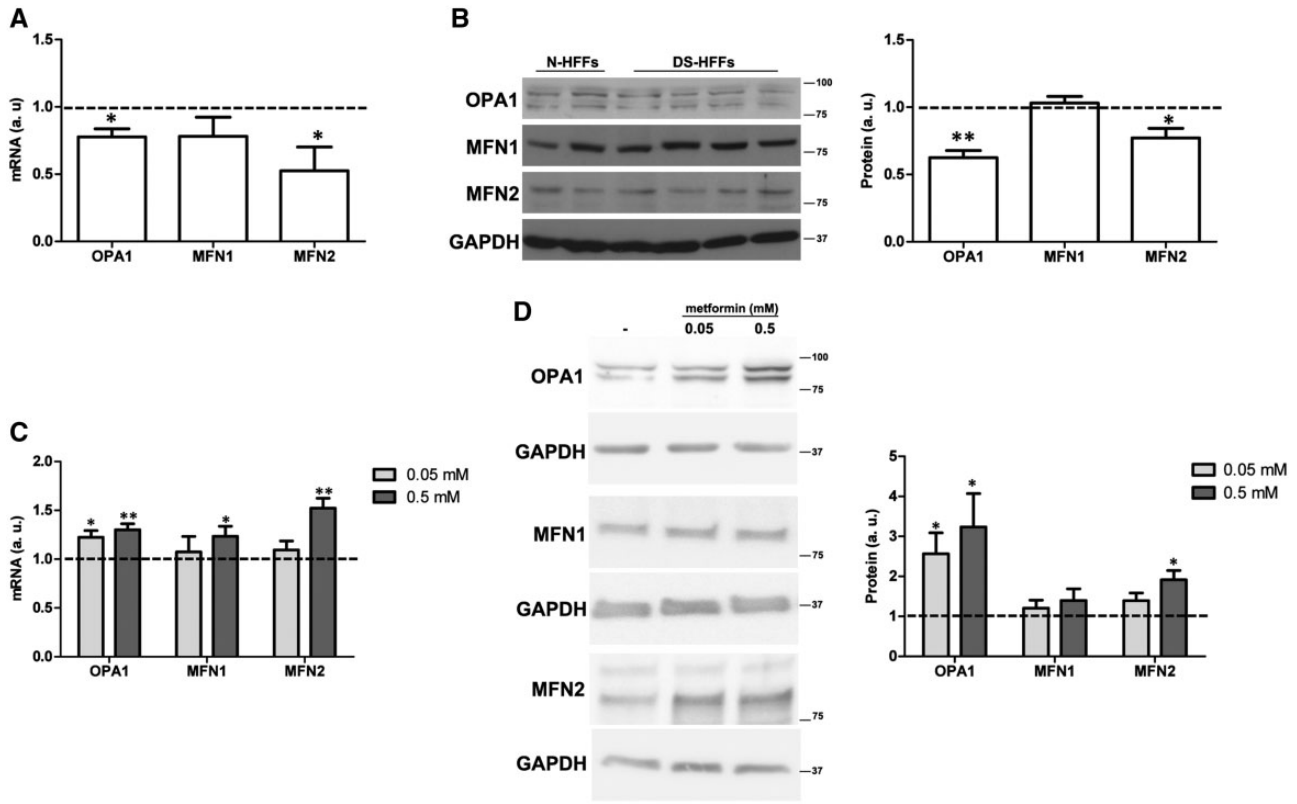

Figure 8. Metformin raises the expression of genes that induce mitochondrial fusion in DS-HFFs. (**A**) *OPA1*, *MFN1* and *MFN2* mRNA expression measured by qRT-PCR upon normalization to a reference gene (*ABELSON*). (**B**) Representative immunoblotting of OPA1, MFN1 and MFN2 and densitometric analysis of three different experiments are shown. GAPDH was measured as a loading control. Unlike *MFN1*, both mRNA and protein levels of *OPA1* and *MFN2*are lower in DS-HFFs versus N-HFFs. Results are expressed as mean values ± SEM of three DS cell cultures compared with H-FFs (set equal to 1). (**C**) *OPA1*, *MFN1* and *MFN2* mRNA expression after 72 h of treatment with metformin and (**D**) representative immunoblotting and densitometric analysis of their protein levels. GAPDH was measured as a loading control. Metformin induces an increase, to a different extent, of the mRNA levels of all three genes. Instead, the protein levels of OPA1 and MFN2, but not of MFN1, are significantly increased upon treatment. Results are expressed as mean values ± SEM of three trisomic cell cultures compared with untreated cells (set equal to 1) in three independent experiments. $^{*}P \leq 0.05$; $^{**}P \leq 0.01$; a.u. = arbitrary units.

reduced growth rates, decreased respiration and a highly heterogeneous mitochondrial population prone to loss of $m\Delta\Psi$ (48).

We analysed the mitochondrial network in trisomic foetal fibroblasts and we observed that it was highly fragmented, with an increased number of shorter mitochondria and a smaller average mitochondrial volume. It is interesting to note that metformin fully restored the mitochondrial network, which became highly branched with an elongated tubular morphology, suggesting that mitochondrial fusion was indeed occurring.

Outer and inner membrane fusion events are co-ordinately coupled, but are mechanistically distinct. Mitofusins are mitochondrial GTPases that likely mediate outer membrane fusion, while the dynamin-related protein OPA1 is required for inner membrane fusion (49). Mitochondrial fusion results in the formation of an interconnected mitochondrial network that allows the mixing and redistribution of proteins and mtDNA. Detailed analysis of fusion-inducing genes in trisomic fibroblasts demonstrated that *MFN2* and *OPA1* were downregulated. Following exposure to 0.5 mM metformin, a significant increase in *OPA1* and *MFN2* mRNA and protein levels was observed. Lower metformin doses were still able to induce mitochondrial fusion without significantly affecting MFNs expression, possibly due to regulatory mechanisms activating these proteins (50) independently of their expression.

A relationship between *PGC-1α* expression and mitochondrial fusion genes has been established. A regulatory pathway involving *PGC-1α*, *ERRα* and *MFN2* drives mitochondrial metabolism by a stimulatory action of *PGC-1α* on the transcription of *MFN2*, via the coactivation of *ERRα* (51). *PGC-1α* silencing induces a decrease in *MFN2* levels in normal pulmonary arterial smooth muscle cells. Conversely, *MFN2* silencing decreases *PGC-1α* levels (52). Furthermore, *MFN2* overexpression causes an increase in *PGC-1α* levels, identifying a bidirectional relationship between *MFN2* and *PGC-1α* expression. Silencing of both genes increases mitochondrial fragmentation in the same cells (52).

Therefore, the *PGC-1α* pathway plays a dual role in regulating mitochondrial function: it positively regulates mitochondrial biogenesis as well as causes organelle remodelling through the induction of *MFN2* transcription (51).

Recent experiments in *Drosophila* also demonstrated a transcriptional relationship between *PGC-1α* and *OPA1* genes. In indirect flight muscles (IFMs) of Drosophila, the nuclear-encoded mitochondrial inner membrane fusion gene, *Opa1-like*, is regulated in a spatiotemporal fashion by the transcription factor/coactivator Erect wing (*Ewg*), the Drosophila homolog of human *NRF-1* (53). The increased expression of *OPA-1* observed upon metformin treatment could co-operate with *MFN2* to restore the mitochondrial network, promoting fusion. In addition to, and independently of its role in mitochondrial fusion, *OPA1*

regulates cristae remodelling by forming oligomers that participate in the cristae junction formation and maintenance (38,54). Its role in the cristae alterations occurring during apoptosis has been well characterized (54–56). Mechanistically, OPA1-dependent stabilization of mitochondrial cristae increases mitochondrial respiratory efficiency and blunts mitochondrial dysfunction, cytochrome c release and ROS production. The OPA1-dependent cristae remodelling pathway is a fundamental, targetable determinant of tissue damage *in vivo* (57). In agreement with these considerations, a higher number of altered mitochondria with abnormal cristae has been observed in trisomic fibroblasts by electron microscopy. Importantly, these alterations were fully reversed by metformin treatment.

Altogether, these data indicate that metformin, by activating the *PGC-1α* pathway, exerts multiple positive effects on mitochondrial activity.

Fusion/fission dynamics and neurodegeneration

Mitochondrial fusion/fission dynamics, and the proteins that control these processes, are ubiquitous. Mitochondrial dynamics play an important role in normal neuronal function and are essential for such neuronal processes as synaptogenesis, Ca^{2+} buffering, axonal transport, and bioenergetics (58). Indeed, alterations of fusion and/or fission processes are primarily associated with severe diseases, notably neurodegenerative diseases such as Alzheimer's, Parkinson's and Huntington's diseases (59–63). A common hallmark of these neurodegenerative diseases, which is also shared with DS, is the impaired function and/or expression of *PGC-1α* (64). From these data in the literature, as well as from our own results on the mitochondrial network organization and on levels of expression of mitochondrial fusion proteins, we speculate that alterations in the fusion/fission dynamics can be relevant in the pathogenesis of DS and that metformin can efficiently counteract these alterations. On the other hand, promoting the expression of *PGC-1α* by the use of metformin might help to correct the abnormal mitochondrial biogenesis, function and dynamics that take place at the early stages of neurodegenerative disorders (65,66).

Conclusions

The results presented here suggest that the use of metformin represents a promising strategy to counteract mitochondrial dysfunction in DS. Its effect is likely due to the transcriptional activation of mitochondria-related genes and to an improvement of mitochondrial network and cristae morphology. Correcting the mitochondrial defect might improve the neurological phenotype and rescue cognitive functions, which are possibly not irreversible, as suggested by the reproducible rescue of learning and memory deficits recently obtained in the DS mouse model Ts65Dn with a large and diverse panel of drugs (40). Metformin treatment might also prevent DS-associated pathologies, such as AD, type 2 diabetes, obesity and hypertrophic cardiopathy, thus providing a better quality of life for DS individuals and their families.

Materials and Methods

Ethics statement

HFFs were obtained from the 'Telethon Bank of Foetal Biological Samples' at the University of Naples. All experimental protocols were approved by the local Institutional Ethics Committee.

Samples

Five skin biopsies were explanted from human foetuses with trisomy of Hsa21 (DS-HFF) and four skin biopsies from euploid foetuses (N-HFF) after therapeutic abortion at 18–22 gestational weeks. Fibroblasts from biopsies were cultured in T25 flasks (BD Falcon) with Chang medium B + C (Irvine Scientific) supplemented with 1% penicillin/streptomycin (Gibco) at 37 °C in a 5% CO_2 atmosphere; all analyses described throughout this study were carried out at cell culture passages 4–5.

Metformin treatment

Metformin hydrochloride (Sigma-Aldrich) was dissolved in water to a stock solution of 100 mM and added to the cell growth medium at the final concentration of 0.05 mM or 0.5 mM. Fresh metformin was added every 24 h for 72 h. In control cells an equal volume of water was added.

RNA extraction and quantitative RT-PCR

Total RNA from each sample was extracted using TRIzol reagent (Gibco/BRL Life Technologies, Inc., Gaithersburg, MD) and was reverse transcribed using the iScript cDNA Synthesis kit (Bio-Rad Laboratories, Inc., Hercules, CA, USA). qRT-PCR was performed using SsoAdvanced universal SYBR Green supermix on a Bio-Rad iCycler CFX96 Touch Real-Time PCR Detection System according to the manufacturer's protocols. Primer pairs (MWG Biotech, Ebersberg, Germany) were designed using the Primer 3 software (http://bioinfo.ut.ee/primer3-0.4.0/primer3; date last accessed 2015)) to obtain amplicons ranging from 100 to 150 base pairs. In order to test primer efficiency, serial dilutions of cDNAs generated from selected samples, which expressed the target genes at a suitable level, were used to generate standard curves for each gene. qRT-PCR results are presented as relative mRNA levels normalized against reference control values. The *ABELSON* housekeeping gene was chosen as reference gene.

Western blotting

After being cultured for three days on plastic dishes, cells were washed twice with ice-cold phosphate-buffered saline (PBS, Hyclone Lab. INC) and lysed in JS buffer (Hepes, pH 7.5, 50 mM, NaCl 150 mM, glycerol 1%, Triton X-100 1%, $MgCl_2$ 1.5 mM, EGTA 5 mM) including protease inhibitor cocktail. Cell lysates were centrifuged at 10,000 *g* for 20 min at 4 °C. Protein concentration was measured by the Lowry or Bradford procedure. Protein extracts were separated by SDS-PAGE and transferred onto nitrocellulose membranes. Membranes were incubated with specific primary antibodies: anti-PGC1α (Calbiochem), anti-GAPDH (Cell Signaling), anti-luciferase (Invitrogen), anti-actin (Sigma), anti-MFN1 (Santa Cruz Biotechnology), anti-MFN2 (Santa Cruz Biotechnology), anti-OPA1 (Santa Cruz Biotechnology). Finally, primary antibodies were detected with the appropriate HRP-conjugated secondary anti-bodies (Santa Cruz Biotechnology or GE-Healthcare) and revealed by chemiluminescence (Pierce) using digital imaging on a Bio-Rad ChemiDoc XRS apparatus or Fuji X-ray film.

Mitochondrial bioenergetics measurements

Real-time measurements of oxygen consumption rate (OCR) were made using an XF^e-96 Extracellular Flux Analyzer (Seahorse Bioscience, Billerica, MA, USA). Cells were plated in

XF^e-96 plates (Seahorse Bioscience) at the concentration of 25,000 cells/well. OCR was measured in XF^e media (non-buffered DMEM medium containing 10 mM glucose, 2 mM L-glutamine and 1 mM sodium pyruvate) under basal conditions and in response to 5 μM Oligomycin, 1.5 μM of carbonyl cyanide-4-(trifluoromethoxy) phenylhydrazone (FCCP) and 1 μM of Antimycin-A and Rotenone (all from Sigma-Aldrich). The key parameters of mitochondrial function were measured. Basal OCR was determined before injections of Oligomycin, the amount of OCR related to ATP production (ATP-linked OCR) was calculated as the difference between basal and Oligomycin-induced OCR and finally, the maximal respiratory capacity was calculated as the difference between the FCCP-stimulated OCR and the OCR after inhibition with Antimycin-A and Rotenone. Each sample was plated at least in triplicate.

Luciferase measurements

The cells were plated on 13-mm diameter glass coverslips for single-sample luminescence measurements and allowed to grow to confluence. To measure total ATP content, the cells were infected with a VR1012-based construct encoding a mitochondrially targeted variant of the Photinuspyralis luciferase under the control of the CMV immediate early promoter (mtLuc), as previously described (67). Cell luminescence was measured in a luminometer constantly perfused with a modified Krebs-Ringer buffer containing: 125 mM NaCl, 5 mM KCl, 1 mM Na_3PO_4, 1 mM $MgSO_4$, 1 mM $CaCl_2$ and 20 μM luciferin. The light output of a coverslip of infected cells was in the range of 10,000–100,000 counts per second (cps) vs a background lower than 1000 cps.

Measurements of mΔΨ

mΔΨ was measured by loading cells with 10 nM tetramethylrhodaminemethyl ester (TMRM; Life Technologies) for 20 min at 37 °C, placed in a humidified chamber at 37 °C and imaged with Nikon Swept Field Confocal microscope (Nikon Instruments Inc.) equipped with a CFI Plan Apo VC60XH objective and an Andor DU885 EM-CCD camera. TMRM excitation was performed at 560 nm and emission was collected through a 590 to 650 nm band-pass filter. TMRM fluorescence was analysed using the NIS Elements software package (Nikon Instruments Inc.). FCCP (10 μM) was added after eight acquisitions to completely collapse the electrical gradient established by the respiratory chain in order to obtain the basal fluorescence values (68). Fluorescence intensity was measured in regions drawn around mitochondria and normalized respect to baseline fluorescence recorded after FCCP.

MitoTracker fluorescence assay

Cells cultured on 12-mm diameter glass coverslips were incubated with 100 nM MitoTracker®RedCMXRos (Molecular Probes) for 20 min in culture medium. After incubation, cells were fixed with 4% paraformaldehyde (Sigma) for 20 min, washed with PBS and then mounted in 50% glycerol in PBS. Nuclei were stained with the DNA intercalating dye DRAQ5 (Bio status, Alexis Corporation). Images were acquired with a Zeiss LSM 510 META confocal laser scanning microscope (Zeiss, Gottingen, Germany) equipped with a plan apo 63x oil-immersion (NA 1.4) objective lens by using two HeNe lasers at 546 and at 633 nm. Fluorescence emission was revealed by a 560–615 band pass filter for MitoTracker®Red and by a 615-long pass filter for DRAQ5. Images were acquired separately in the red and infrared channels at a resolution of 1024 × 1024 pixels, with the confocal pinhole set to one Airy unit, taking Z-slices from the top to the bottom of the cell. Fifty random single cells were analysed for each imaging analysis using a custom script in ImageJ version 1.37.

Mitochondrial morphology analysis

The cells were seeded at a density of 50,000 cells per well onto 25-mm glass coverslips, allowed to grow for 24 h and then infected with mitochondria-targeted GFP inserted into an adenoviral vector (Ad-mtGFP Ex/Em: 495/515). Protein expression was then allowed for 72 h in the presence or absence of metformin. The efficiency of infection was comparable in non-trisomic and trisomic cells both in terms of percentage of GFP positive cells (about 80%) and of intensity of fluorescent GFP signal. Coverslips were placed in an incubated chamber with controlled temperature, CO_2 and humidity. Single cells were imaged, by using the same settings for non-trisomic and trisomic cells, with a Nikon Swept Field Confocal microscope (Nikon Instruments Inc.) equipped with a CFI Plan Apo VC60XH objective and an Andor DU885 EM-CCD camera, which was controlled by NIS Elements 3.2. Fifty-one-plane z-stacks were acquired with voxel dimensions of 133 × 133 × 200 nm (X × Y × Z). The mitochondrial network was then described in numbers of objects, total volume and object volume using the 3D object counter available in the software Fiji (http://www.fiji.sc; date last accessed 2015) (69) while 3D rendering was obtained with the 3D Viewer plugin.

Electron microscopy analysis

Cells were fixed in 1% glutaraldehyde dissolved in 0.2 M HEPES buffer (pH 7.4) for 30 min at room temperature and then post-fixed with a mixture of 2% OsO_4 and 100 mM phosphate buffer (pH 6.8) (1 part 2% OsO_4 plus 1 part 100 mM phosphate buffer) for 25–30 min on ice. Next, the cells were washed three times with water and incubated with 1% thiocarbohydrizide diluted in H_2O for 5 min. Finally, the cells were incubated in a mixture of 2% OsO_4 and 3% potassium ferrocyanide (1 part 2% OsO_4 plus 1 part 3% potassium ferrocyanide) for 25 min on ice and overnight at 4 °C in 0.5% uranyl acetate diluted in H_2O. After dehydration in a graded series of ethanol, the cells were embedded in epoxy resin and polymerized at 60 °C for 72 h. Thin 60-nm sections were cut with a Leica EM UC7 microtome. EM images were acquired from thin sections using an FEI Tecnai-12 electron microscope equipped with a VELETTA CCD digital camera (FEI, Eindhoven, The Netherlands).

The EM analysis was carried out on two euploids and three trisomic cell lines under control conditions and after metformin treatment. The number of damaged mitochondria including any type of ultrastructural changes (partially or completely damaged mitochondria, reduced cristae, broken, shorter or high swollen cristae, giant mitochondria) was calculated as the % of total mitochondria ($n > 60$ per cell line). Similarly, the number of giant mitochondria were counted and expressed as the % of total mitochondria ($n > 60$ per cell line).

The maximal width of cristae was quantified using the ImageJ software line tool (National Institutes of Health, Bethesda, MD, USA) following a previous protocol (34). A line was drawn across the opening between membranes, not including membrane density. Mitochondria were analysed using the

same magnification within a 25-μm square field of view. The width was calculated by averaging the width of 2–4 measurable cristae for each mitochondrion, then averaging the mean value obtained for all mitochondria ($n > 20$) in each sample and in each condition (untreated and treated).

Statistical procedures

Unless otherwise indicated, all assays were performed independently and in duplicate. Statistical analysis was performed using GraphPad Prism software vers.5.0 (GraphPad Software, La Jolla California USA, http://www.graphpad.com; date last accessed 2010). The ANOVA test, with Bonferroni *post hoc* correction in case of multiple comparisons, was applied to evaluate the statistical significance of differences measured throughout the data sets presented. The threshold for statistical significance (p-value) was set at 0.05.

Supplementary Material

Supplementary Material is available at *HMG* online.

Acknowledgements

We thank Sig. Mario Senesi for technical support. We thank the Advanced Microscopy and Imaging facility at the TIGEM institute for the electron microscopy. We thank the PRS PROOFREADING SERVICES for the professionally proofread.

Conflict of Interest statement. None declared.

Funding

POR Campania FSE 2007-2013 Project CREME from Campania Region (to L.N.); POR Campania FSE 2014-2020 from Campania Region (to L.N.).

References

1. Epstein, C.J., Korenberg, J.R., Anneren, G., Antonarakis, S.E., Ayme, S., Courchesne, E., Epstein, L.B., Fowler, A., Groner, Y., Huret, J.L., *et al.* (1991) Protocols to establish genotype-phenotype correlations in Down syndrome. *Am. J. Hum. Genet.*, **49**, 207–235.
2. Jarrold, C., Baddeley, A.D. and Hewes, A.K. (2000) Verbal short-term memory deficits in Down syndrome: a consequence of problems in rehearsal?. *J. Child. Psychol. Psychiatry*, **41**, 233–244.
3. Silverman, W. (2007) Down syndrome: cognitive phenotype. *Ment. Retard. Dev. Disabil. Res. Rev.*, **13**, 228–236.
4. Martin, G.E., Klusek, J., Estigarribia, B. and Roberts, J.E. (2009) Language Characteristics of Individuals with Down Syndrome. *Top. Lang. Disord.*, **29**, 112–132.
5. Shukkur, E.A., Shimohata, A., Akagi, T., Yu, W., Yamaguchi, M., Murayama, M., Chui, D., Takeuchi, T., Amano, K., Subramhanya, K.H., *et al.* (2006) Mitochondrial dysfunction and tau hyperphosphorylation in Ts1Cje, a mouse model for Down syndrome. *Hum. Mol. Genet.*, **15**, 2752–2762.
6. Pallardo, F.V., Lloret, A., Lebel, M., d'Ischia, M., Cogger, V.C., Le Couteur, D.G., Gadaleta, M.N., Castello, G. and Pagano, G. (2010) Mitochondrial dysfunction in some oxidative stress-related genetic diseases: Ataxia-Telangiectasia, Down Syndrome, Fanconi Anaemia and Werner Syndrome. *Biogerontology*, **11**, 401–419.
7. Pagano, G. and Castello, G. (2012) Oxidative stress and mitochondrial dysfunction in Down syndrome. *Adv. Exp. Med. Biol.*, **724**, 291–299.
8. Piccoli, C., Izzo, A., Scrima, R., Bonfiglio, F., Manco, R., Negri, R., Quarato, G., Cela, O., Ripoli, M., Prisco, M., *et al.* (2013) Chronic pro-oxidative state and mitochondrial dysfunctions are more pronounced in fibroblasts from Down syndrome foeti with congenital heart defects. *Hum. Mol. Genet.*, **22**, 1218–1232.
9. Abu Faddan, N., Sayed, D. and Ghaleb, F. (2011) T lymphocytes apoptosis and mitochondrial membrane potential in Down's syndrome. *Fetal. Pediatr. Pathol.*, **30**, 45–52.
10. Aburawi, E.H. and Souid, A.K. (2012) Lymphocyte respiration in children with Trisomy 21. *BMC Pediatr.*, **12**, 193.
11. Arbuzova, S., Hutchin, T. and Cuckle, H. (2002) Mitochondrial dysfunction and Down's syndrome. *Bioessays*, **24**, 681–684.
12. Busciglio, J., Pelsman, A., Wong, C., Pigino, G., Yuan, M., Mori, H. and Yankner, B.A. (2002) Altered metabolism of the amyloid beta precursor protein is associated with mitochondrial dysfunction in Down's syndrome. *Neuron*, **33**, 677–688.
13. Valenti, D., Tullo, A., Caratozzolo, M.F., Merafina, R.S., Scartezzini, P., Marra, E. and Vacca, R.A. (2010) Impairment of F1F0-ATPase, adenine nucleotide translocator and adenylate kinase causes mitochondrial energy deficit in human skin fibroblasts with chromosome 21 trisomy. *Biochem. J.*, **431**, 299–310.
14. Valenti, D., Manente, G.A., Moro, L., Marra, E. and Vacca, R.A. (2011) Deficit of complex I activity in human skin fibroblasts with chromosome 21 trisomy and overproduction of reactive oxygen species by mitochondria: involvement of the cAMP/PKA signalling pathway. *Biochem. J.*, **435**, 679–688.
15. Helguera, P., Seiglie, J., Rodriguez, J., Hanna, M., Helguera, G. and Busciglio, J. (2013) Adaptive downregulation of mitochondrial function in down syndrome. *Cell Metab.*, **17**, 132–140.
16. Mao, R., Wang, X., Spitznagel, E.L., Jr., Frelin, L.P., Ting, J.C., Ding, H., Kim, J.W., Ruczinski, I., Downey, T.J. and Pevsner, J. (2005) Primary and secondary transcriptional effects in the developing human Down syndrome brain and heart. *Genome Biol.*, **6**, R107.
17. Conti, A., Fabbrini, F., D'Agostino, P., Negri, R., Greco, D., Genesio, R., D'Armiento, M., Olla, C., Paladini, D., Zannini, M., *et al.* (2007) Altered expression of mitochondrial and extracellular matrix genes in the heart of human fetuses with chromosome 21 trisomy. *BMC Genomics*, **8**, 268.
18. Izzo, A., Manco, R., Bonfiglio, F., Cali, G., De Cristofaro, T., Patergnani, S., Cicatiello, R., Scrima, R., Zannini, M., Pinton, P., *et al.* (2014) NRIP1/RIP140 siRNA-mediated attenuation counteracts mitochondrial dysfunction in Down syndrome. *Hum. Mol. Genet.*, **23**, 4406–4419.
19. Arron, J.R., Winslow, M.M., Polleri, A., Chang, C.P., Wu, H., Gao, X., Neilson, J.R., Chen, L., Heit, J.J., Kim, S.K., *et al.* (2006) NFAT dysregulation by increased dosage of DSCR1 and DYRK1A on chromosome 21. *Nature*, **441**, 595–600.
20. Quinones-Lombrana, A. and Blanco, J.G. (2015) Chromosome 21-derived hsa-miR-155-5p regulates mitochondrial biogenesis by targeting Mitochondrial Transcription Factor A (TFAM). *Acta Biochim. Biophys.*, **1852**, 1420–1427.
21. Scarpulla, R.C., Vega, R.B. and Kelly, D.P. (2012) Transcriptional integration of mitochondrial biogenesis. *Trends Endocrinol. Metab.*, **23**, 459–466.
22. Jager, S., Handschin, C., St-Pierre, J. and Spiegelman, B.M. (2007) AMP-activated protein kinase (AMPK) action in

skeletal muscle via direct phosphorylation of PGC-1alpha. *Proc. Natl Acad. Sci. U S A*, **104**, 12017–12022.
23. Canto, C. and Auwerx, J. (2009) PGC-1alpha, SIRT1 and AMPK, an energy sensing network that controls energy expenditure. *Curr. Opin. Lipidol.*, **20**, 98–105.
24. Rodgers, J.T., Lerin, C., Haas, W., Gygi, S.P., Spiegelman, B.M. and Puigserver, P. (2005) Nutrient control of glucose homeostasis through a complex of PGC-1alpha and SIRT1. *Nature*, **434**, 113–118.
25. Aatsinki, S.M., Buler, M., Salomaki, H., Koulu, M., Pavek, P. and Hakkola, J. (2014) Metformin induces PGC-1alpha expression and selectively affects hepatic PGC-1alpha functions. *Br. J. Pharmacol.*, **171**, 2351–2363.
26. Wang, J., Gallagher, D., DeVito, L.M., Cancino, G.I., Tsui, D., He, L., Keller, G.M., Frankland, P.W., Kaplan, D.R. and Miller, F.D. (2012) Metformin activates an atypical PKC-CBP pathway to promote neurogenesis and enhance spatial memory formation. *Cell Stem Cell*, **11**, 23–35.
27. Salomaki, H., Vahatalo, L.H., Laurila, K., Jappinen, N.T., Penttinen, A.M., Ailanen, L., Ilyasizadeh, J., Pesonen, U. and Koulu, M. (2013) Prenatal metformin exposure in mice programs the metabolic phenotype of the offspring during a high fat diet at adulthood. *PLoS One*, **8**, e56594.
28. Labuzek, K., Suchy, D., Gabryel, B., Bielecka, A., Liber, S. and Okopien, B. (2010) Quantification of metformin by the HPLC method in brain regions, cerebrospinal fluid and plasma of rats treated with lipopolysaccharide. *Pharmacol. Rep.*, **62**, 956–965.
29. Hofer, A., Noe, N., Tischner, C., Kladt, N., Lellek, V., Schauss, A. and Wenz, T. (2014) Defining the action spectrum of potential PGC-1alpha activators on a mitochondrial and cellular level in vivo. *Hum. Mol. Genet.*, **23**, 2400–2415.
30. Chen, Y., Wang, Y., Chen, J., Chen, X., Cao, W., Chen, S., Xu, S., Huang, H. and Liu, P. (2012) Roles of transcriptional corepressor RIP140 and coactivator PGC-1alpha in energy state of chronically infarcted rat hearts and mitochondrial function of cardiomyocytes. *Mol. Cell. Endocrinol.*, **362**, 11–18.
31. Scarpulla, R.C. (2011) Metabolic control of mitochondrial biogenesis through the PGC-1 family regulatory network. *Acta Biochim. Biophys.*, **1813**, 1269–1278.
32. Zick, M., Rabl, R. and Reichert, A.S. (2009) Cristae formation-linking ultrastructure and function of mitochondria. *Acta Biochim. Biophys.*, **1793**, 5–19.
33. Cogliati, S., Frezza, C., Soriano, M.E., Varanita, T., Quintana-Cabrera, R., Corrado, M., Cipolat, S., Costa, V., Casarin, A., Gomes, L.C., *et al.* (2013) Mitochondrial cristae shape determines respiratory chain supercomplexes assembly and respiratory efficiency. *Cell*, **155**, 160–171.
34. Lavatelli, F., Imperlini, E., Orru, S., Rognoni, P., Sarnataro, D., Palladini, G., Malpasso, G., Soriano, M.E., Di Fonzo, A., Valentini, V., *et al.* (2015) Novel mitochondrial protein interactors of immunoglobulin light chains causing heart amyloidosis. *Faseb J.*, **29**, 4614–4628.
35. Davies, V.J., Hollins, A.J., Piechota, M.J., Yip, W., Davies, J.R., White, K.E., Nicols, P.P., Boulton, M.E. and Votruba, M. (2007) Opa1 deficiency in a mouse model of autosomal dominant optic atrophy impairs mitochondrial morphology, optic nerve structure and visual function. *Hum. Mol. Genet.*, **16**, 1307–1318.
36. Chan, D.C. (2012) Fusion and fission: interlinked processes critical for mitochondrial health. *Annu. Rev. Genet.*, **46**, 265–287.
37. Labbe, K., Murley, A. and Nunnari, J. (2014) Determinants and functions of mitochondrial behavior. *Annu. Rev. Cell Dev. Biol.*, **30**, 357–391.
38. Frezza, C., Cipolat, S., Martins de Brito, O., Micaroni, M., Beznoussenko, G.V., Rudka, T., Bartoli, D., Polishuck, R.S., Danial, N.N., De Strooper, B., *et al.* (2006) OPA1 controls apoptotic cristae remodeling independently from mitochondrial fusion. *Cell*, **126**, 177–189.
39. Zick, M., Duvezin-Caubet, S., Schafer, A., Vogel, F., Neupert, W. and Reichert, A.S. (2009) Distinct roles of the two isoforms of the dynamin-like GTPase Mgm1 in mitochondrial fusion. *FEBS Lett.*, **583**, 2237–2243.
40. Gardiner, K.J. (2015) Pharmacological approaches to improving cognitive function in Down syndrome: current status and considerations. *Drug Des. Devel. Ther.*, **9**, 103–125.
41. Fritah, A., Steel, J.H., Nichol, D., Parker, N., Williams, S., Price, A., Strauss, L., Ryder, T.A., Mobberley, M.A., Poutanen, M., *et al.* (2010) Elevated expression of the metabolic regulator receptor-interacting protein 140 results in cardiac hypertrophy and impaired cardiac function. *Cardiovasc. Res.*, **86**, 443–451.
42. Ryan, M.T. and Hoogenraad, N.J. (2007) Mitochondrial-nuclear communications. *Annu. Rev. Biochem.*, **76**, 701–722.
43. Ventura-Clapier, R., Garnier, A. and Veksler, V. (2008) Transcriptional control of mitochondrial biogenesis: the central role of PGC-1alpha. *Cardiovasc. Res.*, **79**, 208–217.
44. Bambrick, L.L. and Fiskum, G. (2008) Mitochondrial dysfunction in mouse trisomy 16 brain. *Brain Res.*, **1188**, 9–16.
45. Gavalda-Navarro, A., Villena, J.A., Planavila, A., Vinas, O. and Mampel, T. (2014) Expression of adenine nucleotide translocase (ANT) isoform genes is controlled by PGC-1alpha through different transcription factors. *J. Cell. Physiol.*, **229**, 2126–2136.
46. Klingenberg, M. (2008) The ADP and ATP transport in mitochondria and its carrier. *Acta Biochim. Biophys.*, **1778**, 1978–2021.
47. Valenti, D., de Bari, L., de Rasmo, D., Signorile, A., Henrion-Caude, A., Contestabile, A. and Vacca, R.A. (2016) The polyphenols resveratrol and epigallocatechin-3-gallate restore the severe impairment of mitochondria in hippocampal progenitor cells from a Down syndrome mouse model. *Acta Biochim. Biophys.*, **1862**, 1093–1104.
48. Chen, H., Chomyn, A. and Chan, D.C. (2005) Disruption of fusion results in mitochondrial heterogeneity and dysfunction. *J. Biol. Chem.*, **280**, 26185–26192.
49. Zhang, Y. and Chan, D.C. (2007) New insights into mitochondrial fusion. *FEBS Lett.*, **581**, 2168–2173.
50. Wiedemann, N., Stiller, S.B. and Pfanner, N. (2013) Activation and degradation of mitofusins: two pathways regulate mitochondrial fusion by reversible ubiquitylation. *Mol. Cell*, **49**, 423–425.
51. Soriano, F.X., Liesa, M., Bach, D., Chan, D.C., Palacin, M. and Zorzano, A. (2006) Evidence for a mitochondrial regulatory pathway defined by peroxisome proliferator-activated receptor-gamma coactivator-1 alpha, estrogen-related receptor-alpha, and mitofusin 2. *Diabetes*, **55**, 1783–1791.
52. Ryan, J.J., Marsboom, G., Fang, Y.H., Toth, P.T., Morrow, E., Luo, N., Piao, L., Hong, Z., Ericson, K., Zhang, H.J., *et al.* (2013) PGC1alpha-mediated mitofusin-2 deficiency in female rats and humans with pulmonary arterial hypertension. *Am. J. Respir. Crit. Care Med.*, **187**, 865–878.
53. Rai, M., Katti, P. and Nongthomba, U. (2014) Drosophila Erect wing (Ewg) controls mitochondrial fusion during muscle

growth and maintenance by regulation of the Opa1-like gene. *J. Cell Sci.*, **127**, 191–203.
54. Pernas, L. and Scorrano, L. (2016) Mito-Morphosis: Mitochondrial Fusion, Fission, and Cristae Remodeling as Key Mediators of Cellular Function. *Annu. Rev. Physiol.*, **78**, 505–531.
55. Cogliati, S., Enriquez, J.A. and Scorrano, L. (2016) Mitochondrial Cristae: Where Beauty Meets Functionality. *Trends Biochem. Sci.*, **41**, 261–273.
56. MacVicar, T. and Langer, T. (2016) OPA1 processing in cell death and disease - the long and short of it. *J. Cell Sci.*, **129**, 2297–2306.
57. Varanita, T., Soriano, M.E., Romanello, V., Zaglia, T., Quintana-Cabrera, R., Semenzato, M., Menabo, R., Costa, V., Civiletto, G., Pesce, P., *et al.* (2015) The OPA1-dependent mitochondrial cristae remodeling pathway controls atrophic, apoptotic, and ischemic tissue damage. *Cell Metab.*, **21**, 834–844.
58. Oettinghaus, B., Schulz, J.M., Restelli, L.M., Licci, M., Savoia, C., Schmidt, A., Schmitt, K., Grimm, A., More, L., Hench, J., *et al.* (2016) Synaptic dysfunction, memory deficits and hippocampal atrophy due to ablation of mitochondrial fission in adult forebrain neurons. *Cell Death Differ.*, **23**, 18–28.
59. Hroudova, J., Singh, N. and Fisar, Z. (2014) Mitochondrial dysfunctions in neurodegenerative diseases: relevance to Alzheimer's disease. *Biomed. Res. Int.*, **2014**, 175062.
60. Itoh, K., Nakamura, K., Iijima, M. and Sesaki, H. (2013) Mitochondrial dynamics in neurodegeneration. *Trends Cell Biol.*, **23**, 64–71.
61. Reddy, P.H. (2014) Misfolded proteins, mitochondrial dysfunction, and neurodegenerative diseases. *Acta Biochim. Biophys.*, **1842**, 1167.
62. Van Laar, V.S. and Berman, S.B. (2013) The interplay of neuronal mitochondrial dynamics and bioenergetics: implications for Parkinson's disease. *Neurobiol. Dis.*, **51**, 43–55.
63. Bertholet, A.M., Delerue, T., Millet, A.M., Moulis, M.F., David, C., Daloyau, M., Arnaune-Pelloquin, L., Davezac, N., Mils, V., Miquel, M.C., *et al.* (2016) Mitochondrial fusion/fission dynamics in neurodegeneration and neuronal plasticity. *Neurobiol. Dis.*, **90**, 3–19.
64. Rona-Voros, K. and Weydt, P. (2010) The role of PGC-1alpha in the pathogenesis of neurodegenerative disorders. *Curr. Drug Targets*, **11**, 1262–1269.
65. Xavier, J.M., Rodrigues, C.M. and Sola, S. (2015) Mitochondria: Major Regulators of Neural Development. *Neuroscientist*, **22,** 346–358.
66. Campello, S. and Scorrano, L. (2010) Mitochondrial shape changes: orchestrating cell pathophysiology. *EMBO Rep.*, **11**, 678–684.
67. Porcelli, A.M., Pinton, P., Ainscow, E.K., Chiesa, A., Rugolo, M., Rutter, G.A. and Rizzuto, R. (2001) Targeting of reporter molecules to mitochondria to measure calcium, ATP, and pH. *Methods Cell Biol.*, **65**, 353–380.
68. Patergnani, S., Giorgi, C., Maniero, S., Missiroli, S., Maniscalco, P., Bononi, I., Martini, F., Cavallesco, G., Tognon, M. and Pinton, P. (2015) The endoplasmic reticulum mitochondrial calcium cross talk is downregulated in malignant pleural mesothelioma cells and plays a critical role in apoptosis inhibition. *Oncotarget*, **6**, 23427–23444.
69. Schindelin, J., Arganda-Carreras, I., Frise, E., Kaynig, V., Longair, M., Pietzsch, T., Preibisch, S., Rueden, C., Saalfeld, S., Schmid, B., *et al.* (2012) Fiji: an open-source platform for biological-image analysis. *Nat. Methods*, **9**, 676–682.